University of Copenhagen

Niels Bohr Institute

Black Holes and Gravitational Waves

Jose María Ezquiaga

(jose.ezquiaga@nbi.ku.dk)

Last Modification: May 16, 2024

Contents

Prelude

These lecture notes are very much under construction. They will be updated regularly. Please bear with me!

A few points before we get started:

Throughout the lectures notes I will use different **conventions** for units. The general principle is that whenever some dimensionfull number needs to be computed, I will include all the Gs, cs and $\hbar$s. When this is not the case, typically during analytical derivations, I will set $c = 1$. I will try to keep G and $\hbar$. I will also try to avoid using too many **acronyms** in different chapters, but if you get lost in the next page you can find a compilation of all acronyms. Similarly, I will try to add relevant **references** to both seminal works and recent results. Given the amount of literature I will certainly miss many works though. Citations are not meant to be exhaustive but rather indicative. You can find the full bibliography at the end of the lecture notes.

Exercises will be marked with boxes within the text of each chapter. For instance:

Exercise 0.1: An example exercise

The content of the example exercise to do

The list of all exercises can be found at the end of the document. The exercise sheet for evaluation will be sent separately.

This course is short and the field of black holes and gravitational waves very rich and active nowadays. Therefore we will inevitably only cover some basic points and highlights of current research lines. In the lectures notes I invite you to **explore** further some other topics. Those will be marked in boxes, both to excite you but mostly to identify them as separate from the standard curriculum. An example:

Explore: An example topic

An example text for further exploration

Since these parts are outside of the main curriculum, I will add further details as we move along. This means, keep checking previous chapters for new edits.

Enjoy the course!

Acronyms

AGN active galactic nucleus. 17

BH black hole. 1

EHT Event Horizon Telescope. 17

EM electromagnetic. 17

EoS equation of state. 4

FRW Friedman-Robertson-Walker. 6

GR general relativity. 1

GW gravitational wave. 18

NS neutron star. 8

PBH primordial black hole. 7

PISN pair instability supernova. 12

SMBH super massive black hole. 14

TOV Tolman–Oppenheimer–Volkoff. 4, 11

WD white dwarf. 8

CHAPTER

1

Black holes in our Universe: how they form, how we find them

Black holes (BHs) are incredible predictions of general relativity (GR). From a theoretical perspective, they are unique objects to explore the limits of GR. What it is more impressive though is that over the past decades we have accumulated overwhelming evidence of their existence. Therefore, black holes are no longer only a theoretical playground to push the limit of our theories, but rather an actual laboratory where we can test different predictions. In this chapter we are going to have a *brief overview* of how black holes form in our Universe and the different evidence that we have about their existence. By its own nature, this will be a chapter that will cover very different physical phenomena. Therefore, instead of providing detailed derivations we will focus mostly on highlighting the key processes and their order of magnitude implications.

1.1 Gravitational Collapse

In simple terms, in order to form a black hole we need to accumulate enough energy-density in a small enough region so that the gravitational pull cannot be stopped by any other force. In the astrophysical context such dense regions essentially only occur in stars. There, the battle is between the pressure and the gravity of its interior. We are going to take a glimpse of how this looks like in realistic astrophysical set up in Sec. 1.2. For the moment we will focus on understanding some general principles.

We aim to study the gravitational collapse of a spherically symmetric star. Irrespectively of the material properties of the interior, Birkhoff's theorem guarantees us that outside of the star (i.e. in vacuum) the metric is described by the Schwarzschild metric:

$$ds^2 = -\left(1 - \frac{r_{\rm Sch}}{r}\right) dt^2 + \left(1 - \frac{r_{\rm Sch}}{r}\right)^{-1} dr^2 + r^2 d\Omega^2 \,, \tag{1.1.1}$$

where

$$r_{\rm Sch} = \frac{2GM}{c^2} \simeq 3 \left(\frac{M}{M_\odot}\right) {\rm km} \,, \tag{1.1.2}$$

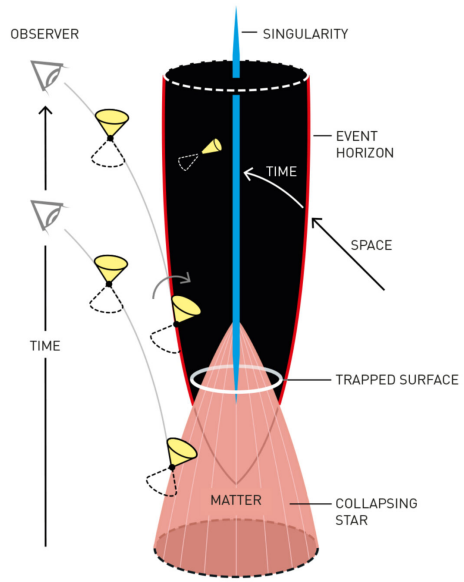

Figure 1.1. Schematic diagram of star collapsing into a black hole Credit Johan Jarnestad/The Royal Swedish Academy of Science.

with $M_\odot$ being the mass of the Sun. Since the interior and the exterior solutions must match, we can understand the behavior at the surface of the star following geodesics of Schwarzschild geometry.[1] For example, we can ask how the light emitted at the surface of the collapsing star would be seen by a distant observer. This light would be redshifted by

$$z = \frac{\Delta\lambda}{\lambda} \propto e^{t/2t_{\rm Sch}} \tag{1.1.3}$$

where the crossing time of the Schwarzschild radius is

$$t_{\rm Sch} = \frac{r_{\rm Sch}}{c} = \frac{2GM}{c^3} \simeq 10 \left(\frac{M}{M_\odot}\right) \mu{\rm s}\,. \tag{1.1.4}$$

The redshift increases exponentially with a characteristic time scale of $2t_{\rm Sch}$. The luminosity of the emitted light will also decay at this rate. Therefore, for an external observer, the light emitted by the star will dim at an incredible high rate for astrophysical standards. For a 1 solar mass star, the characteristic decaying time of the luminosity is only 20μs. A schematic representation of the collapse into a black hole is given in Fig. 1.1.

[1] Recall this was covered in detail in Troel's course and lecture notes.

Exercise 1.1: The light from a collapsing star

Consider a comoving distant observer at a fixed spatial position around a collapsing star. Show that the radiation emitted at the surface of the star redshifts exponentially at late times. In other words, derive Eq. (1.1.3).

We now wish to study the interior of the star.[2] We will consider the simplest possible composition for the interior: a perfect fluid. Its energy momentum tensor is described by

$$T^{\mu\nu} = (\rho + p)U^\mu U^\nu + p g^{\mu\nu} \,. \tag{1.1.5}$$

where ρ is the energy density and p the pressure of the fluid. U^μ is the local four velocity. We assume also a static, spherically symmetric, interior metric

$$ds^2 = -A(r)dt^2 + B(r)dr^2 + r^2 d\Omega^2 \,. \tag{1.1.6}$$

The fact that we are choosing a static solution implies that the fluid cannot flow, $U^i = 0$. Taking U^μ pointing in the timelike direction, the normalization condition $U_\mu U^\mu = -1$ fully fixes it to $U^0 = A^{-1/2} = -1/U_0$. Altogether explicitly:

$$U_\mu = (-A^{1/2}, 0, 0, 0) \,, \tag{1.1.7}$$

and, as a consequence,

$$T_{\mu\nu} = \mathrm{diag}(A \cdot \rho, B \cdot p, r^2 \cdot p, r^2 \sin^2\theta \cdot p) \,. \tag{1.1.8}$$

With the metric and the energy-momentum tensor one can solve the field equations

$$G_{\mu\nu} = R_{\mu\nu} - \frac{1}{2} R g_{\mu\nu} = 8\pi G T_{\mu\nu} \,. \tag{1.1.9}$$

Because of all our assumptions, only the diagonal terms are relevant. In fact, only one of the two angular equations is independent, $G_{\phi\phi} = \sin^2\theta G_{\theta\theta}$, and we are left with three couple equations to solve.[3]

Inspired by Schwarzschild geometry, one can define a new radial-dependent mass function $\mathcal{M}(r)$

$$B(r)^{-1} \equiv 1 - \frac{2G\mathcal{M}(r)}{r} \,. \tag{1.1.10}$$

Inserting this definition in the tt equation, we find

$$\frac{d\mathcal{M}(r)}{dr} = 4\pi r^2 \rho(r) \,, \tag{1.1.11}$$

[2] I follow Carroll's Chapter 5.8 [1] and Zee's VII.4 [2].

[3] You are welcome to derive the Einstein equations for this metric and energy-momentum tensor by hand! If interested in learning a Mathematica package designed for tensorial calculations I have left a notebook example in the course materials.

which can be integrate to find

$$\mathcal{M}(r) = 4\pi \int_0^r dr' r'^2 \rho(r') \,. \tag{1.1.12}$$

For a star of radius R, the matching conditions with the exterior metric imply that

$$M = \mathcal{M}(R) = 4\pi \int_0^R dr r^2 \rho(r) \,, \tag{1.1.13}$$

so the mass function $\mathcal{M}(r)$ that we introduced can be interpreted as the mass within a radius r. It is interesting to point out however, that this does not match with the integration of the energy-density ρ over a spatial volume element, $\gamma_{ij} dx^i dx^j$, specifically

$$\tilde{M} = \int_{r<R} \rho(r) \sqrt{\gamma} d^3x = 4\pi \int_0^R \rho(r) B(r) r^2 dr = 4\pi \int_0^R \frac{\rho(r) r^2}{\sqrt{1 - \frac{2G\mathcal{M}(r)}{r}}} dr \,. \tag{1.1.14}$$

The difference between the two is due to the gravitational binding energy arising from the gravitational attraction of the fluid within the star:

$$E_B = \tilde{M} - M > 0 \,. \tag{1.1.15}$$

Back to the field equations, using the radial equation and the energy-momentum conservation $\nabla_\mu T^{\mu\nu} = 0$ (instead of the $\phi\phi$-equation), which for a perfect fluid and a static spherically symmetric metric takes a very simple form

$$\frac{dp}{dr} = -(\rho + p) \frac{d \ln A^{1/2}}{dr} \,, \tag{1.1.16}$$

one can eliminate the $A(r)$ metric component to arrive at the *Tolman–Oppenheimer–Volkoff (TOV) equation*

$$\frac{dp}{dr} = -\frac{G\mathcal{M}(r)\rho(r)}{r^2} \left(1 + \frac{p(r)}{\rho(r)}\right) \left(1 + \frac{4\pi r^3 p(r)}{\mathcal{M}(r)}\right) \left(1 - \frac{2G\mathcal{M}(r)}{r}\right)^{-1} \tag{1.1.17}$$

describing hydrostatic equilibrium. For a given equation of state (EoS) $p = p(\rho)$, the TOV equation together with the interior mass equation (1.1.12) can be used to solve $p(r)$ and $\rho(r)$. These set of couple equations generically require numerical integration except for simplified scenarios as we will check next. Before that, plugging the TOV equation (1.1.17) back to the energy-momentum conservation (1.1.16), we can fully solve for the interior metric

$$\frac{d \ln A^{1/2}}{dr} = \frac{G\mathcal{M}(r)}{r^2} \left(1 + \frac{4\pi r^3 p(r)}{\mathcal{M}(r)}\right) \left(1 - \frac{2G\mathcal{M}(r)}{r}\right)^{-1} \,. \tag{1.1.18}$$

We can check that the matching conditions with the exterior geometry are also correct, since at the surface $\mathcal{M}(R) = M$ and $p(R) = 0$ and the above equation can be easily

integrated to obtain $A = 1 - \frac{r_{\rm Sch}}{r}$. Finally, it is interesting to point out that in the non-relativistic limit the TOV equation reduces to Newton's equation for stellar interiors:

$$\frac{dp}{dr} = -\frac{G\mathcal{M}(r)\rho(r)}{r^2}\,. \tag{1.1.19}$$

This equation just corresponds to the balance between the gravitational force and the radial pressure.

1.1.1 A star of constant density

Now that have an equation for the interior of the star, we wish to solve it in order to understand the conditions for collapse. We choose a simple model that allows us to inegrate the TOV equation analytically, that is an *incomprehensible fluid* of constant density

$$\rho(r < R) = \rho_*\,, \qquad \rho(r > 0) = 0\,. \tag{1.1.20}$$

Then, the interior mass is simply

$$\mathcal{M}(r) = \frac{4\pi r^3}{3}\rho_*\,, \tag{1.1.21}$$

with the density defined by the mass and radius of the star $\rho_* = M/(4\pi R^3/3)$. The TOV equation can be solve to find

$$p(r) = \rho_* \frac{\left(1 - \frac{r_{\rm Sch}}{R}\right)^{1/2} - \left(1 - \frac{r^2 r_{\rm Sch}}{R^3}\right)^{1/2}}{\left(1 - \frac{r^2 r_{\rm Sch}}{R^3}\right)^{1/2} - 3\left(1 - \frac{r_{\rm Sch}}{R}\right)^{1/2}}\,, \tag{1.1.22}$$

whose density profile is plotted in the left panel of Fig. 1.2. The pressure increases as one approaches the center of the star $r \to 0$. Moreover, the central pressure $p(0)$ increases as the star becomes more compact. This is plotted in the right panel of Fig. 1.2. In fact, when reaching $R = 9r_{\rm Sch}/8$ the central pressure diverges. This highlights that there is a limit to how compact a constant density star can be in order to have a static solution. In other words, there is a maximum mass that a spherically symmetric star can have in order to have a static solution:

$$M < \frac{8}{9}\frac{R}{r_{\rm Sch}} \simeq 3\left(\frac{R}{10{\rm km}}\right) M_\odot\,. \tag{1.1.23}$$

If a shrinking star reaches this critical radius, then it will continue shrinking and eventually collapse into a black hole when $R < r_{\rm Sch}$. Although this important results was derived for a rather specific EoS, Buchdahl's theorem [3] states that this result holds for any "reasonable" EoS.

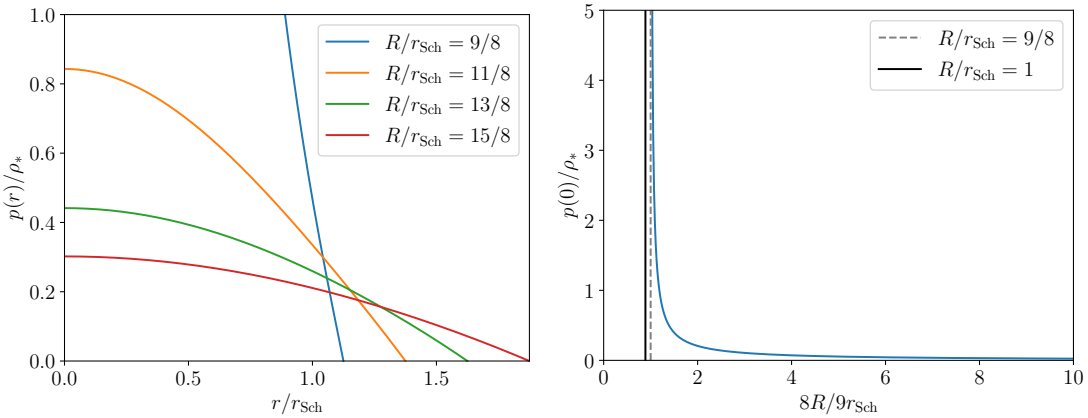

Figure 1.2. On the left, pressure profile in the radial component for a spherically star of radius R made of an incompressible perfect fluid of density ρ_*. On the right, pressure at the center as a function of the star's radius.

1.1.2 A universe within a star

Before moving on to gravitational collapse in realistic stars, we are going to adventure in a small digression. This is motivated by the remarkable similarities between the (simplified) set up that we have considered for the interior of a star and the geometry of the Universe at large scales as described by a Friedman-Robertson-Walker (FRW) metric:

$$ds^2 = -dt^2 + a(t)^2 d\vec{x}^2 \,, \tag{1.1.24}$$

where $a(t)$ is the scale factor. In fact, in order to study the background expansion of the Universe one also models matter as a perfect fluid. However, instead of assuming a static, spherically symmetric metric as in the interior of the star, one assumes a homogeneous and isotropic time varying metric.

Let us consider the case of a universe filled with a cosmological constant $\rho = \Lambda$ with EoS $p = -\Lambda$. The field equations then reduce to $R_{\mu\nu} = 8\pi G\Lambda g_{\mu\nu}$ (noting that $R = 32\pi G\Lambda$). A cosmological constant directly leads to a mass profile of

$$\mathcal{M}(r) = \frac{4\pi r^3}{3}\Lambda \,. \tag{1.1.25}$$

The interior metric can be obtained solving Eq. (1.1.18), which after inputting our ansatzs looks like

$$\frac{d\ln A}{dr} = \frac{-2H^2 r}{1 - H^2 r^2} \,, \tag{1.1.26}$$

where we have defined $H^2 = 8\pi G\Lambda/3$ in resemblance of the Hubble parameter $H = d\ln a/dt$. This equation can be solved to obtain $A(r) = 1 - H^2 r^2$. From Eq. (1.1.10) one then obtains $B = 1/A$. Altogether, the spherically symmetric static metric that solves for a cosmological constant is

$$ds^2 = -(1 - H^2 r^2)dt^2 + (1 - H^2 r^2)^{-1} dr^2 + r^2 d\Omega^2 \,. \tag{1.1.27}$$

In a cosmological setup of a universe filled with a cosmological constant solving the Friedman equation

$$\left(\frac{d\ln a}{dt}\right)^2 = \frac{8\pi G}{3}\Lambda = H^2 \tag{1.1.28}$$

leads to a exponentially increasing scale factor $a \propto e^{Ht}$. Back to the FRW metric this is

$$ds^2 = -dt^2 + e^{2Ht}d\vec{x}^2\,, \tag{1.1.29}$$

which is nothing but a de Sitter space-time. Therefore, the interior of a star is mathematically equivalent to an expanding universe.

Exercise 1.2: A ball of dust

Let's consider an even simpler model (perhaps the simplest) for the interior of a star: a spherically symmetric pressureless fluid of constant density, i.e. a "ball of dust". This is also known as the Oppenheimer-Snyder model [4]. Because there are no pressure forces, the dust particles in the surface of the star follow radial geodesics. Following what you have learned so far, study the gravitational collapse of this model. To what cosmology is this model equivalent to?

Explore: black hole formation in the early universe

Although astrophysically we typically only think of stars as dense enough environments to trigger gravitational collapse into a black hole, cosmologically there are other options. In particular, black holes could form directly from the collapse of curvature fluctuations ζ in the early Universe. The fraction of black holes forming β is typically postulated in terms of the probability of having a fluctuation beyond a given threshold

$$\beta = \int_{\zeta_{\rm thr}}^{\infty} p(\zeta)d\zeta\,, \tag{1.1.30}$$

where $p(\zeta)$ is the probability density function. The mass of the black hole that forms is proportional to the size of the causal horizon that is collapsing. Large curvature fluctuations can be produced during inflation. Such fluctuations may collapse upon reentry. Their mass is therefore associated to the epoch in which the fluctuations are generated counted as the number of e-folds N:

$$M_{\rm pbh} \sim 4\pi\gamma\frac{M_{\rm pl}}{H_{\rm inf}}e^{2N}\,, \tag{1.1.31}$$

where $M_{\rm pl}$ is the reduced Planck mass, $H_{\rm inf}$ is the energy scale of inflation, and γ is efficiency parameter encapsulating the details of the gravitational collapse, typically $\gamma \sim 0.2$. Black holes formed in the early Universe are typically referred as *primordial black holes (PBHs)*. The range of masses of PBHs is therefore subject to the details of the concrete inflationary model. There are also other mechanisms different from inflation that could produce PBHs. A famous one is cosmic strings.

1.2 Stellar graveyard: white dwarfs, neutron stars and black holes

In the last section we have studied a generic process of gravitational collapse in a simplified toy model. Now we wish to explore a bit what are the actual stellar remnants that can form in our Universe and what is their interplay with the other fundamental forces apart form gravity. A detailed derivation of such processes goes beyond the scope of this course and here we only aim to draw the main arguments and relevant scales.

Different to other celestial bodies such as planets whose structure is supported by material pressures, stars are sustained by thermonuclear power. Starting from Hydrogen, the core of the stars converts lighter elements into heavier ones by fusion emitting heat that supports its structure. When the nuclear fuel is used (after iron the binding energy per nucleon decreases, meaning that heavier elements cannot release the extra energy needed to compensate the additional gravity due to the contraction), there are two options: *i)* the star reaches equilibrium again due to non-thermal forces or *ii)* the star continues gravitational collapse. The most relevant non-thermal pressure is associated to the Pauli exclusion principle that prevents fermions to occupy the same (quantum) state, also known as Fermi pressure.

When a star is supported by the Fermi pressure of electrons then it is a *white dwarf (WD)*. When a star is supported by the Fermi pressure of neutrons it is a *neutron star (NS)*. Beyond Fermi pressure and nuclear forces there are no other source of energy to prevent the gravitational collapse. Therefore, once one passes the support of NS one end up with a BH. This is why when we think about the remnants of stars, referred sometimes as the *stellar graveyard*, these are WDs, NSs and BHs. A schematic diagram of the different routes of stellar evolution is presented in Fig. 1.3. Something that we did mention though is that through this process of collapse, there could be instabilities triggered that will end up in runaway processes leading to explosion. These are of course the *supernovas*.

Explore: Boson stars

As we have seen the Fermi pressure is a basic ingredient to balance the gravitational pull and form stable stars when the object is composed of fermions. Matter in the standard model of particle physics is made of fermions, so this should cover it all. However, there could be additional fundamental particles of bosonic type. How then a stable configuration could be form? The key is self-interaction and the simplest example is a complex scalar field [5].

1.2.1 Maximum mass of white dwarfs

We now wish to investigate a bit further the stability of WDs.[4] As explained above, these are stars that are supported by the Fermi pressure of the electrons. The gravity,

[4] I follow Hartle's chapters 12.1 and 24 [6].

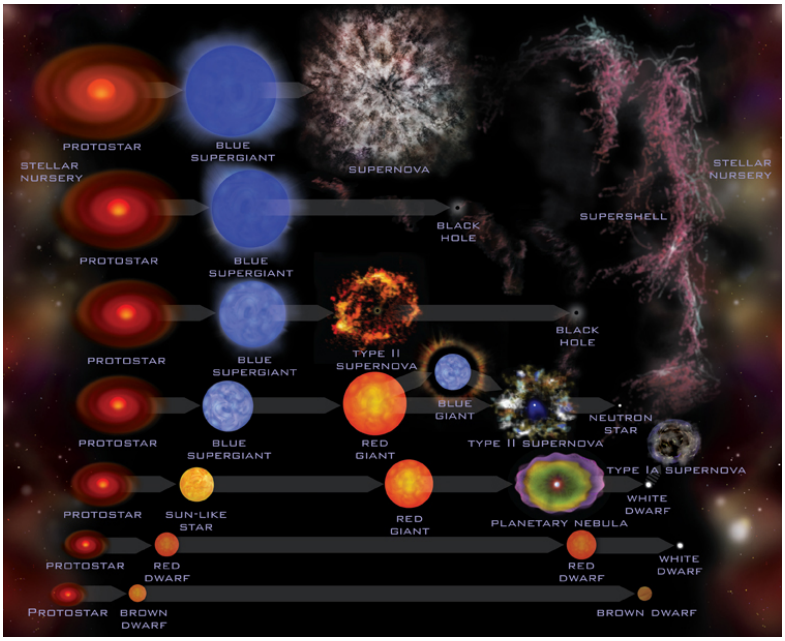

Figure 1.3. Schematic diagram of the different outcomes of stellar evolution. Image credit Chandra.

on the other hand, is driven by the mass of the nuclei ($m_e \ll m_p, m_n$). The balance between these two forces determine the stability of a WD for different configurations. In particular, we are interested in finding what is the maximum mass for which the electron Fermi pressure can no longer counterbalance the gravity, i.e. the maximum mass of a WD.

To get a taste of the problem we are first going to do a rough estimate. We assume a spherically symmetric star of radius R made of A electrons. To ensure neutrality we take A protons. Since electrons cannot occupy the same state, we can think of their wavelength λ as associated to their number density within star, $n_e \sim A/R^3$. This corresponds to a scaling of $\lambda \sim R/A^{1/3}$. The more compact the star is, the larger the frequency and therefore energy and momentum:

$$p \sim \hbar/\lambda \sim A^{1/3}\hbar/R\,. \tag{1.2.1}$$

Assuming that the electrons have been compressed enough to be relativistic, $E = \sqrt{p^2c^2 + m_e^2c^4} \approx pc$, the total Fermi energy is roughly

$$E_F \sim A(pc) \sim A^{4/3}\hbar c/R\,. \tag{1.2.2}$$

This energy is compensated by the gravitational interaction driven by the protons

$$E_G \sim -G(m_p A)^2/R\,. \tag{1.2.3}$$

The total energy is $E_T = E_F + E_G$ and scales as $1/R$. For a sufficient number of electrons A within a radius R then the gravitational energy wins. This determines a

critical number of electrons

$$A_{\rm crit} \sim \left(\frac{\hbar c}{G m_p^2}\right)^{3/2} \sim 10^{57} \tag{1.2.4}$$

(recall $2\pi\hbar = 6.62 \cdot 10^{-34}$Js, $G = 6.67 \cdot 10^{-11}$Nm^{2}kg^2, $c = 3 \cdot 10^8$m/s and $m_p = 1.7 \cdot 10^{-27}$kg) which in turns defines a critical mass

$$M_{\rm crit} \sim m_p A_{\rm crit\sim} \sim M_\odot \,. \tag{1.2.5}$$

(recall $M_\odot = 2 \cdot 10^{30}$kg) . Therefore, WDs cannot be much heavier than the Sun.

A more detailed analysis follows from solving the TOV equation (1.1.17). Modeling the star with a given EoS, one can find the maximum mass that can be supported. This is precisely what Chandrasekhar discovered [7]. Therefore, the maximum WD mass is known as the *Chandrasekhar limit*.

In order to solve this problem we are only missing to define the EoS of the WD. For a completely degenerate electron gas (see details in [6]) this can be found in the nonrelativistic to be

$$p = \frac{1}{5}(3\pi^2)^{3/2}\left(\frac{\hbar^2}{m_e}\right) n_e^{5/3} \,, \tag{1.2.6}$$

while in the relativistic one

$$p = \frac{1}{4}(3\pi^2)^{1/3}\,(\hbar c)\, n_e^{4/3} \,, \tag{1.2.7}$$

where, again, n_e is the number density of electrons. This is sometimes written in terms of the number of protons Z and nucleons A, to give the energy density ρ

$$n_e = \frac{Z}{A}\frac{\rho}{m_H c^2} \,, \tag{1.2.8}$$

where m_H is the mass of the hydrogen. Putting together the last two equations one then gets an EoS: $p = p(\rho)$. EoS are sometimes parametrized in terms

$$\gamma \equiv \frac{\rho + p}{p}\frac{dp}{d\rho} \,, \tag{1.2.9}$$

a dimensionless quantity measuring the stiffness of an EoS. For degenerate fermions in the nonrelativistic limit $\gamma = 5/3$, smoothly transitioning towards $\gamma = 4/3$ as they become relativistic. Larger γ means more increase in pressure with increases in the energy density.

For a given central density ρ_c, the TOV equations can be integrated from the center $p(\rho_c)$ to the radius of the star $p(R) = 0$. Exploring all possible central densities ρ_c, from 0 to ∞, allows to determine the family of spherical stars made of matter with the assumed EoS. The final product is a set of allowed masses $M(\rho_c)$ and radii $R(\rho_c)$ for this type of stars. An example of the solutions of the TOV equations is given in Fig.

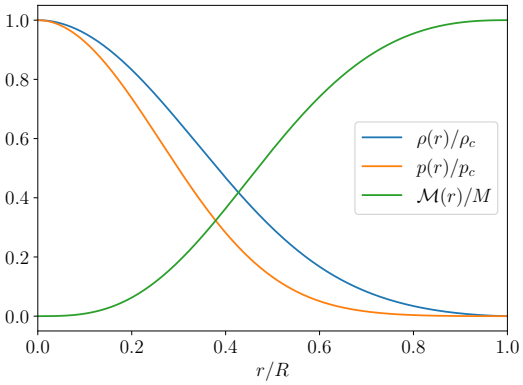

Figure 1.4. The stellar structure for a star with a equation of state with stiffness parameter $\gamma = 5/3$ obtained solving the Tolman–Oppenheimer–Volkoff (TOV) equations (1.1.17. M and R are the mass and radius of the star as obtained from solving the TOV equations.

1.4. Both the pressure and density steadily decrease from their central value to 0 at the sruface of the star, R. The mass does the opposite: increasing from 0 to M.

For WDs it turns out the maximum mass is $\sim 1.4 M_\odot$ with a radius of 1000 km for densities of about 10^{11}g/cm^3. Roughly, WDs have the mass of the Sun within the size of the Earth. This is a very compact object, but still mostly in the the Newtonian regime,

$$\frac{GM_{\rm wd}}{c^2 R_{\rm wd}} \sim \text{few} \times 10^{-3} \tag{1.2.10}$$

For higher densities to 10^{11}g/cm^3, there are other relevant physical phenomena that we study next.

Exercise 1.3: Finding hydrostatic equilibrium

Solve the TOV equations (numerically) to find the maximum mass of stars with different equations of state $p = p_c(\rho/\rho_c)^\gamma$. To do so it is convenient to rewrite the TOV equations in terms of dimensionless variables $\tilde\rho = \rho/\rho_c$, $\tilde p = p/p_c$, $\tilde r = r/R$ and $\tilde{\mathcal{M}} = \mathcal{M}/M$. Note that both M and R need to be obtained from the solutions themselves, but giving an initial guess serves to simplify the numerical implementation.

1.2.2 Maximum mass of neutron stars

We are now going to study the case of stars more dense than WDs. Recall that for WDs we are dealing with a star with free electrons and nuclei (this roughly occurs at $\rho \gtrsim 10^4\text{g/cm}^3$). As the star becomes more compact, electrons become relativistic ($m_e c^2 \simeq 0.5\text{MeV}$) at about $\rho \sim 10^6\text{g/cm}^3$. Soon after it becomes energetically favorable to convert electrons and protons into neutrons releasing neutrinos:

$$e^- + p^+ \to n + \nu_e\,. \tag{1.2.11}$$

This occurs at energies $\sim m_n c^2 - m_p c^2 \simeq 1.3\text{MeV}$. As the density increases, the star becomes more and more neutron rich. At around $\rho \sim 4 \cdot 10^{11}\text{g/cm}^3$ the most energetic neutrons become unbound from nuclei. Eventually, all neutrons are free forming a fluid sometimes refered as neutron matter. This is the material of which NSs are made of.

Studying the maximum mass of NSs could be done in a similar fashion to what we have done for WDs. Neutrons are also fermions and therefore are equally subject to the Fermi pressure which mass be compensated by the gravitational pull. Differently though, the gravitational energy is also provided by the neutrons themselves. The main difficulty however of studying NSs is the fact that one could reach densities in which nuclear interactions become relevant. This is a very active field of research, trying to understand how the matter within NSs behaves.

The first attempts to set this maximum mass were done by Tolman [8] and Oppenheimer–Volkoff [9] in what is now known as the *Tolman–Oppenheimer–Volkoff limit* in analogy to the Chandrasekhar limit. (Much) Later studies including nuclear interactions have set the maximum mass at around $2M_\odot$ for non-rotating NSs and about $3M_\odot$ for rapidly rotating ones [10]. A typical NS has a mass of $1.4M_\odot$ for a radius of about 10km. Therefore

$$\frac{GM_{\text{ns}}}{c^2 R_{\text{ns}}} \sim \text{few} \times 10^{-1} \tag{1.2.12}$$

which is 100 times the case of WDs. For NSs, relativistic effects at the surface can become important. For scale, a NS has about the mass of the Sun within the size of the urban area of Copenhagen.

Explore: Stellar-origin black hole maximum mass and the pair instability supernovae

We have just seen that there are fundamental processes in nature that prevent white dwarfs and neutron stars to form more massive than a given value. Is there a similar limit for black holes?
In fact, there is. If the core of the star is massive enough it reach energies in which it is possible to produce electron and positrons. This pair production is sourced by high energy gamma rays that no longer help supporting the star against gravity, reducing temporarily the pressure. This photon pressure reduction can makes the star compress. This can lead to a runaway process in which the higher energy of the photons leads to more pair production. Eventually, if this instability continues the star ends up in a supernova in what is known as *pair instability supernova (PISN)* [11]. The explosion ejects so much material that a massive remnant black hole cannot be formed. This process is subject to many details about stellar evolution and the composition of the star, but it is thought that it would prevent stellar-origin black holes to form above $\sim 50M_\odot$. Interestingly, for very heavy stars (which are expected to be rare on the other hand), this instability is insufficient to prevent the collapse of the star into a black hole. Therefore, it is possible that heavier black holes above $\sim 120M_\odot$ could form. This leads to the interesting

observational prospect that there is a gap in the mass spectrum of stellar-origin black holes. This is sometimes called the PISN or upper mass gap. This theory is actively being probed with gravitational wave observations.
As an aside, one should note that this only refers to the direct formation of black holes from stars. Black holes of larger masses can form due to accretion or black hole mergers as we will see later. Moreover, in the context of primordial black holes it is also possible to directly collapse curvature perturbations into more massive black holes.

Explore: Is there a black hole minimum mass?

From stellar evolution (recall Fig. 1.3) we have seen that black holes only form for stars more compact that a NS. Does this mean that astrophysically black holes smaller than $1-3M_\odot$ cannot be formed? Well... this depends on the type of matter that the star is made of, but for "standard" configurations (i.e. material within the standard model of particle physics) this is the case.
But still, what is the minimum mass of black hole forming from a star. 2, 3, 4 solar masses? This is a complicated question that requires simulating accurately the collapse of a star. Observationally, there is an interesting fact. With X-ray binaries in the Milky Way (we will talk more about this in 1.3.3) there have been observations of black holes with only $> 5M_\odot$ [], while neutron star masses are $< 3M_\odot$ as discussed before. This is sometimes referred as the *neutrons star - black hole mass gap* or *lower mass gap* when referring to all the compact binaries collectively. Interestingly, with gravitational waves there has been recently the observation of a compact object with mass between $2.5-4.5M_\odot$ [], squarely within this purported gap. More observation will tell if there is a new population down there!
On a different note, as argued before, in the early universe it is "easy" to form black holes of any mass. Therefore, detecting sub-solar mass black holes have been though as a smoking gun for primordial black holes. If they are too small, they would however evaporate by emission of Hawking radiation.

1.3 Evidence for black holes

Since any light that falls into a black hole cannot escape, by its own nature black holes are difficult to observe. However, evidence for the existence of black holes can be obtained in several indirect ways. Essentially, the whole game is being able to weight the object and demonstrate that the mass enclosed in such volume can only be explained by a black hole. In this section we wish to make a rapid tour around these different pieces of evidence. This is not meant to be exhaustive or self-contained, but rather an invitation to explore more and a validation of the fact that nowadays we are pretty sure black holes exist in Nature.

1.3.1 Astrometry

Astrometry is the branch of astronomy dedicated to precisely measuring the position and velocities of stars. Within our galaxy, where most precise measurements are possible, observing the motion of stars has turn out to be a prolific way of finding black holes of different masses. Perhaps most well known is the study of "S stars" around Sagittarius A* (SgrA*), the super massive object at the galactic center of the Milky Way.

Before diving into the center of our galaxy, let us refresh some scales. A typical galaxy weights around $10^{12} M_\odot$. It is composed (essentially) of dark matter and stars, which form a bulge of about $10^{10} M_\odot$. Typical sizes for the bulge (which is the part that we can observe directly!) are around a few kiloparsec (recall 1pc $\simeq 3 \cdot 10^{16}$m). It is thought that typical galaxies host a super massive black hole (SMBH) of between 10^6 and $10^9 M_\odot$. The Schwarzschild radius of such object can be as large as $\sim 10^9$km, but this is only $\sim 10^{-4}$pc. Therefore the size of the SMBH in the center of the galaxy is much smaller than the size of the galaxy. This makes very challenging to resolve such small scales for distant galaxies.

For our own Galaxy, different observatories have been tracking the trajectories of the closest stars to SgrA* for decades, cf. Fig. 1.5. These trajectories are described by Newtonian mechanics so that the velocity at different positions serves to bound the total mass within the orbit. Current observations determine $M_{\text{SgrA}^*} \sim 4 \cdot 10^6 M_\odot$ [12]. These amazing observations were recognized with the Nobel prize in 2020 to Andrea Ghez and Reinhard Genzel as leaders of the competing teams.

Explore: Gaia black holes

Gaia, a European space mission, aims to map a billion stars in our Galaxy. Its precision in positioning stars is unprecedented, making it the perfect instrument for astrometry. In particular, by monitoring the trajectories of so many stars it is well positioned to find the rare cases in which a star forms a binary with a dormant black hole. These systems are very hard to detect otherwise do to the lack of additional electromagnetic emission by the black hole. There has been so far three black holes discovered in Gaia data [13–15].

1.3.2 Gravitational lensing

GR predicts that both the propagation of massive and massless particles are affected by the gravitational interaction with other objects. This means that in the same way that celestial bodies modify their trajectories according to the curvature of space-time, electromagnetic radiation can be deflected by massive objects which act as *gravitational lenses*. In fact, the deflection of light observed during the solar eclipse of 1919 was an impactful experimental test of GR. In the weak filed limit, the deflection angle produced

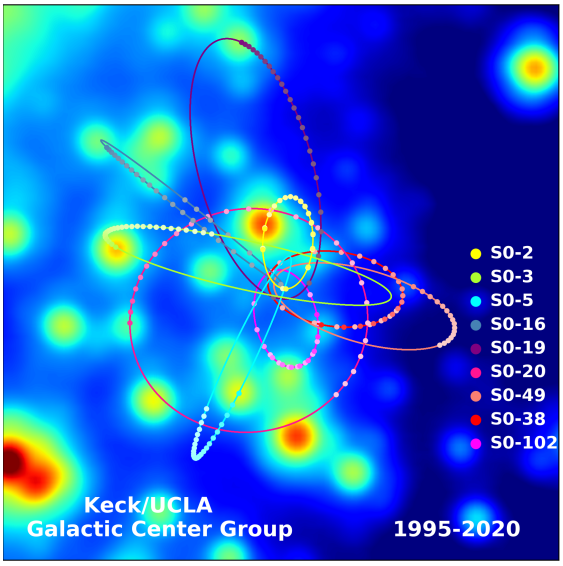

Figure 1.5. The orbits of stars within the central 1.0 × 1.0 arcseconds of our Galaxy. In the background, the central portion of a diffraction-limited image taken in 2015 is displayed. While every star in this image has been seen to move over the past 20 years, estimates of orbital parameters are best constrained for stars that have been observed through at least one turning point of their orbit. The annual average positions for these stars are plotted as colored dots, which have increasing color saturation with time. Also plotted are the best fitting simultaneous orbital solutions. Credit: plot and caption from UCLA Galactic Center Group.

by a compact lens is given by[5]

$$\Delta\alpha \sim \frac{4GM_L}{bc^2} = 2\frac{r_{\rm Sch}}{b}\,, \tag{1.3.1}$$

where M_L is the mass of the lens and b the impact parameter. For example, for our Sun which has $R_\odot \simeq 7\cdot 10^5$km, a light ray passing by its surface will be deflected by $\sim 10^{-5}$ radians or ~ 2 arcsec.

Such a point lens will also have the effect of magnifying any foreground source. The angular scale at which lensing becomes relevant is

$$\theta_E = \sqrt{\frac{4GM_L}{c^2}\frac{D_{LS}}{D_L D_S}}\,, \tag{1.3.2}$$

where D_L, D_S and D_{LS} are respectively the (angular diameter) distances from the observer to the lens, to the source and between the lens and the source. For short wavelengths compared to the size of the lens, a point lens always produces two images ($\pm$) and their positions and magnifications can be solved analytically, in particular

$$\mu_\pm = \frac{b^2+2}{2b\sqrt{b^2+4}} \pm \frac{1}{2}\,. \tag{1.3.3}$$

[5]Recall this was described in detail in Troel's course and lecture notes.

When the two images cannot be resolved, an observer is only sensitive to the total flux

$$\mu_{\rm tot} = |\mu_+| + |\mu_-| = \frac{b^2+2}{b\sqrt{b^2+4}}\,. \tag{1.3.4}$$

As $b \to 0$, the magnification diverge. This means that if we are a distant source and a lens passes by then the flux of source is expected to increased significantly over a period of time. It is to be noted that the magnification does not diverge in reality, it is just a consequence of our approximations of small wavelengths and points sources. Those are eventually broken in reality due to either the finite size of the wavelength or the finite size of the source, whatever is larger. Still, the magnifications can be very large for a point lens and a point source

$$\mu_{\rm max} \sim \pi t_{\rm Sch}\omega \simeq 4\cdot 10^5 \left(\frac{M_L}{M_\odot}\right)\left(\frac{f}{\rm GHz}\right)\,, \tag{1.3.5}$$

where f is the frequency of the wave. When the source has a size of $R_{\rm src}$, the maximum magnification is

$$\mu_{\rm max} = \left(1+4\frac{R_E}{R_{\rm src}}\right)^{1/2}\,, \tag{1.3.6}$$

where $R_E = D_L\theta_E$ is the Einstein radius of the lens.

Since it is typically difficult to know the intrinsic luminosity of a given source, the total magnification is not such a informative parameter. However, the time variability of the magnification is more robust, as this depends more directly on the source-lens configuration and not the knowledge of the source properties. In particular, to know the relevant time scale we want to compute how long the source will be within the Einstein radius of the lens. If we denote v the relative velocity between the lens and the source, this time scale is simply

$$t_\mu = \frac{R_E}{v} \simeq 0.2{\rm yr}\left(\frac{200{\rm km/s}}{v}\right)\left(\frac{M_L}{M_\odot}\right)^{1/2}\left(\frac{D_L}{10{\rm kpc}}\right)^{1/2}\left(\frac{D_{LS}}{D_S}\right)\,. \tag{1.3.7}$$

Therefore, for solar-mass compact lenses with typical velocities of hundreds of kilometers per second within our galaxy the duration of the magnification is of the order of a fraction of a year. Larger lenses are therefore more challenging to constrain as one needs to monitor the source for longer time. In essence this was the idea of Paczynski, who proposed this as a method to map stellar mass compact objects in our Galaxy [16]. Different surveys have pursued this search such as MACHO, EROS and most recently OGLE. The best candidate to date for an isolated black hole using this lensing method is OGLE-2011-BLG-0462.

Exercise 1.4: Gravitational telescopes

Due to the effect of gravitational lensing, structures in the universe can become "gravitational telescopes" magnifying distant objects. Black hole are among the

most efficient lenses. They are also the simplest as they can be described by point lenses. For a universe filled of black holes of the same mass, compute the probability that a source is amplified with a magnification larger than 10.

1.3.3 Electromagnetic emission

Due to the large gravitational attraction around a black hole, any surrounding material that is being accreted can experience significant accelerations, heating up and emitting electromagnetic (EM) radiation. The key to identify such source of radiation as a black hole is to demonstrate that no other object could source such amount of power in such a small region.

It has been known since the 1960s that there are extremely bright quasi-stellar objects at large distances [17]. These quasi-stellar objects, also known as *quasars*, are particularly surprising because of their small size (this is why initially they were confused with stars) and high luminosity. A Quasar is nowadays understood as very luminous active galactic nucleus (AGN). Quasar luminosities can be 10^4 times brighter than the luminosity of all stars in a galaxy. Therefore, in the most distant cases, only the quasar itself and not the host galaxy is observable. The energy powering these powerful quasars is thought to come from the gravitational binding energy liberated during the accretion as well as the EM extraction of the rotational energy of the BH.

At a much smaller scale, a BH that form in a binary star system can also lead to significant EM emission. Note that 2/3 of all stars are members of binary systems! If one of them undergoes a supernova to end up in a BH, then trajectory of the companion star will be affected and new effects will arise. In particular there could be a periodic lensing of the star. However, more importantly, the BH can accrete the star emitting large amounts of energy. Binary systems discovered in this way are known as *X-ray binaries* because of the observed frequencies. Many X-ray binaries have been identified in the galaxy. However, not all of them contain a BH since, as we have seen before, WDs and NSs are also natural stellar remanents. Therefore, the key for identifying a BH within a X-ray binary is to be able to measure its mass and, in particular, to prove that it is larger than $\gtrsim 3M_\odot$. This can be (partially) done thanks to the Doppler shift of the radial velocity which contains information about the masses in the binary. With additional information about the mass of the star, which can be estimated from its spectrum if it is a common star, then the mass of the potential BH can be inferred.

Explore: Imaging a black holes

Although a direct image of the black hole interior is not possible, one can hope to construct a telescope with enough resolution to see in detail the surroundings of a black hole down to the photon ring, the last stable photon orbit. This is precisely what the Event Horizon Telescope (EHT) is set to do through very-long-baseline interferometry. And, of course, they did it! We have now pictures of black holes, in particular the one in our own Galaxy and in our closest neighbor, Andromeda.

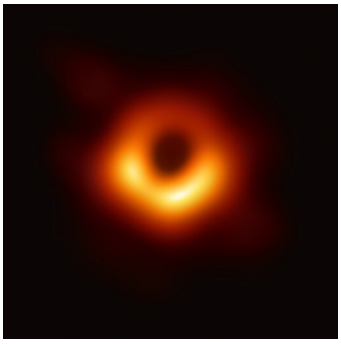

Figure 1.6. Image of the supermassive black hole at the center of our neighbor galaxy, Messier 87, captured by the Event Horizon Telescope [18].

The image of the later is presented in Fig. 1.6 where one can see the expected ring like structure. The actual size of the inner ring and its relation to the photon ring is an active area of research since its detectability with current telescopes is subject to the details of the accretion disk around the black hole. In any case, this observation already serves to measure the mass of the black hole in a completely independent way. This measurement is most interesting for the black hole in our Galaxy as we have precise astrometric measurements to compare with.

1.3.4 Binary coalescence

When two black holes encounter with each other and collide, they perturb the spacetime around them producing gravitational waves (GWs) that travel across the cosmos. These waves encode information about the masses of the binary and its shape is a firm prediction of GR.

The frequency of these waves is correlated with the orbital motion of the binary. As the black holes approach each other they orbit in a faster way. It is easy to guess that the amplitude of the wave will be larger when the black holes are about to merge (and therefore also easier to detect!). For a binary of similar masses, an order of magnitude of the frequency of a GW around merger time can be obtained by considering that is should inversely proportional to the Schwarzschild crossing time of both hole. This rough approximation shows that

$$f \sim \frac{1}{2\pi}\frac{1}{2t_{\rm Sch}} \sim 800{\rm Hz}\left(\frac{10M_\odot}{M}\right) . \tag{1.3.8}$$

Therefore black holes of tens of solar masses will merge with frequencies of hundreds of Hz (this is much larger than any electromagnetic transient!). Similarly, if we expect that spacetime close to merger leads to a distortion of order one, an order of magnitude estimate of the amplitude h leads to

$$h \sim \mathcal{O}(1)\frac{r_{\rm Sch}}{r} \sim 10^{-23}\left(\frac{1{\rm Gpc}}{r}\right)\left(\frac{M}{10M_\odot}\right) . \tag{1.3.9}$$

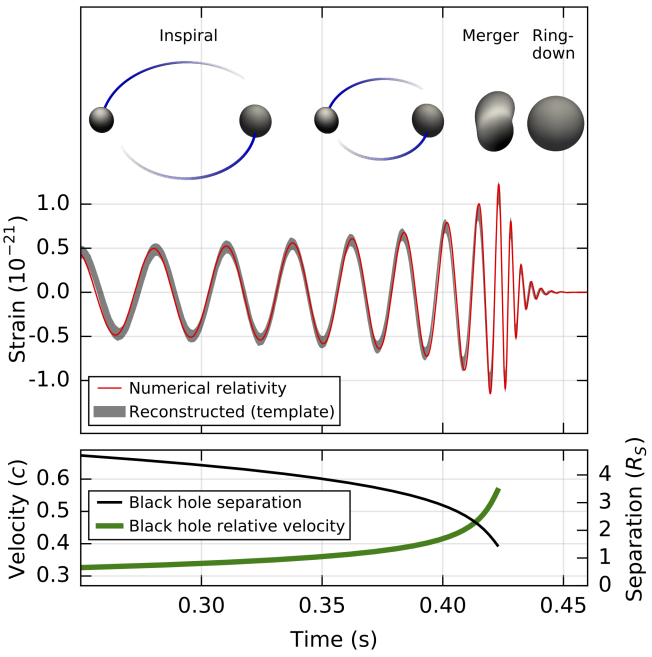

Figure 1.7. GW150914, the first detection of a binary black hole merger [19]. The top panel shows the strain as a function of time. The lower panel shows the relative velocity and separation of the objects as they merge. The velocity is a fraction of the speed of light, c, and the separation just a few Schwarzschild radius, R_S. For more details about the first GW detection, see the science summary.

In words, black holes of tens of solar masses merging at cosmological distances will have very small amplitudes in our detectors.

The waveform of the first GW detected is presented in Fig. 1.7. On the top panel one can see the time domain waveform with its characteristic insparal, merger and ring-down phases. This was a binary of $\sim 30M_\odot$ merging at ~ 400Mpc. The merger frequency was about 250Hz. On the bottom panel one can see the orbital separation and the velocity. As the black holes are about to merge they are moving almost at the speed of light!

These binary coalescences are fascinating and their study will be the focus of the rest of the course.

List of exercises

Bibliography

[1] S. M. Carroll, *Spacetime and Geometry: An Introduction to General Relativity*. Cambridge University Press, 7, 2019.

[2] A. Zee, *Einstein Gravity in a Nutshell*. Princeton University Press, New Jersey, 5, 2013.

[3] H. A. Buchdahl, *General relativistic fluid spheres*, *Phys. Rev.* **116** (Nov, 1959) 1027–1034.

[4] J. R. Oppenheimer and H. Snyder, *On continued gravitational contraction*, *Phys. Rev.* **56** (Sep, 1939) 455–459.

[5] R. Ruffini and S. Bonazzola, *Systems of selfgravitating particles in general relativity and the concept of an equation of state*, *Phys. Rev.* **187** (1969) 1767–1783.

[6] J. B. Hartle, *Gravity: An introduction to Einstein's general relativity*. 2003.

[7] S. Chandrasekhar, *The maximum mass of ideal white dwarfs*, *Astrophys. J.* **74** (1931) 81–82.

[8] R. C. Tolman, *Static solutions of einstein's field equations for spheres of fluid*, *Phys. Rev.* **55** (Feb, 1939) 364–373.

[9] J. R. Oppenheimer and G. M. Volkoff, *On massive neutron cores*, *Phys. Rev.* **55** (Feb, 1939) 374–381.

[10] V. Kalogera and G. Baym, *The maximum mass of a neutron star*, *Astrophys. J. Lett.* **470** (1996) L61–L64, [astro-ph/9608059].

[11] W. A. Fowler and F. Hoyle, *Neutrino Processes and Pair Formation in Massive Stars and Supernovae*, *Astrophys. J. Suppl.* **9** (1964) 201–319.

[12] A. M. Ghez et al., *Measuring Distance and Properties of the Milky Way's Central Supermassive Black Hole with Stellar Orbits*, *Astrophys. J.* **689** (2008) 1044–1062, [arXiv:0808.2870].

[13] K. El-Badry et al., *A Sun-like star orbiting a black hole*, *Mon. Not. Roy. Astron. Soc.* **518** (2023), no. 1 1057–1085, [arXiv:2209.06833].

[14] K. El-Badry et al., *A red giant orbiting a black hole*, *Mon. Not. Roy. Astron. Soc.* **521** (2023), no. 3 4323–4348.

[15] **Gaia** Collaboration, P. Panuzzo et al., *Discovery of a dormant 33 solar-mass black hole in pre-release Gaia astrometry*, arXiv:2404.10486.

[16] B. Paczynski, *Gravitational microlensing by the galactic halo*, *Astrophys. J.* **304** (1986) 1–5.

[17] M. Schmidt, *3C 273 : A Star-Like Object with Large Red-Shift*, *Nature* **197** (1963), no. 4872 1040.

[18] **Event Horizon Telescope** Collaboration, K. Akiyama et al., *First M87 Event Horizon Telescope Results. I. The Shadow of the Supermassive Black Hole*, *Astrophys. J. Lett.* **875** (2019) L1, [arXiv:1906.11238].

[19] **LIGO Scientific, Virgo** Collaboration, B. P. Abbott et al., *Observation of Gravitational Waves from a Binary Black Hole Merger*, *Phys. Rev. Lett.* **116** (2016), no. 6 061102, [arXiv:1602.03837].